Thermochimica Acta, 230 (1993) 167–175
Elsevier Science Publishers B.V., Amsterdam
SSDI 0040-6031(93)01174-2

Structural and acidic properties of cationic-exchanged Y and mordenite zeolites

Mohamed Mokhtar Mohamed

Chemistry Department, Faculty of Science, Al-Azhar University, Cairo (Egypt)

(Received 5 March 1993; accepted 22 March 1993)

Abstract

The catalytically important high-silica zeolites NaSPM, NaLPM and NaY, which had been exchanged with different metal cations, Cu, Ni and Co, were examined through ammonia desorption by differential scanning calorimetry.

The acidity of the different zeolite samples was investigated and correlated to the framework and structural alterations following cation exchange.

The activation energy values for the different zeolite samples were obtained and these values were found to be in the order NaSPM > NiSPM > CuSPM > CuLPM and Cu–Y ≫ Ni–Y.

The heats of reaction of NH_3 on NaSPM were slightly lower than those on NiSPM, whereas those for Cu–Y were much higher than those for Ni–Y.

INTRODUCTION

Zeolites exhibit specific ion exchange properties which often differ from those found in other organic or inorganic exchangers. Although the zeolitic ion exchange is complicated by simultaneous processes such as swelling of the exchanger phase, absorption of non-electrolytes and salt imbibition, their exchange properties have been studied in great detail. Moreover, the high electric field and structural rigidity are negligibly influenced in zeolites when concentrations are less than 1 N.

The incorporation of transition metals in zeolites is commonly used in catalyst preparation. These metals may be used in their cationic form [1] but they are also often reduced to metallic clusters [2, 3] or used in combination with ligands forming a complex [4]. Adsorption of organic or inorganic molecules can also alter the properties of a zeolite [5, 6].

It is, however, imperative that the applied molecules have strong interactions with the surface. Both internal and external surface modifications have been observed. In particular, the introduction of transition metal ions into the zeolite lattice seems to be very interesting because these ions exhibit catalytic activity in homogeneous as well as heterogeneous catalysis

[7]. Therefore, ion exchange studies are important from both a practical and a fundamental point of view.

Several research groups [8, 9] have investigated the exchange properties of monovalent and divalent metal ions in siliceous zeolites. Whereas, monovalent ions reveal complete exchange ($M^+/Al = 1.0$), the ion exchange properties for divalent metal ions are less clear and, in general, incomplete exchange is found. Therefore, our aim is to investigate the acidity of Y zeolite, and of large-port and small-port mordenite zeolites, modified with different divalent metal ions, by means of differential scanning calorimetry. The difference in reactivity of the modifying agents towards the three substrates is explained with reference to their structural properties and ion exchange behaviour, which give supplementary information on the acidic nature of these modified substrates.

EXPERIMENTAL

The mordenite samples investigated in this study were Na large-port mordenite (NaLPM), obtained from the Norton Co., England, under the registered trade name Zeolon 900 and a small-port mordenite (NaSPM), supplied by La Societe Chimique de la Grand Paroisse (SCGP), France. Samples of Na–Y zeolite were supplied by Linde Union Carbide. The compositional characteristics of the zeolites used in this work are listed in Table 1.

All the zeolite samples were ion exchanged with transition metal ions (Co^{2+}, Cu^{2+} and Ni^{2+}) in their aqueous nitrate solutions by taking 100 g of the zeolite sample and refluxing with 400 cm^3 of the nitrate solution, the concentration of which was chosen on the basis that the exchange procedure is approx. 80% efficient in obtaining the desired exchange level. The pH of the nitrate solution was kept at approx. 6. The zeolite was

TABLE 1

Compositional characteristics of NaLPM, NaSPM and Y zeolites used in this work

	NaLPM [a]	NaSPM [a]	Na–Y [b]
Morphology	20–50 mesh	3 mm pellets	60–100 mesh
Binder	None	None	None
Na content (AAS)/mmol per g dry wt.	2.35 ± 0.05	2.42 ± 0.04	11.12 ± 0.02
Al content (EDTA titr.)/ mmol per g dry wt.	2.37 ± 0.06	2.42 ± 0.04	10 ± 0.03
Si/Al ratio (^{27}Si-NMR)	4.6	4.6	2.4
Water content (gravimetry)/wt.%	13.0 ± 0.2	13.1 ± 0.2	24.79

[a] The mordenite data are taken from ref. 10; Na–Y[b] data are deduced from this work.

filtered and washed thoroughly with hot deionized water, then oven-dried at 373 K for a further 24 h to accomplish a redistribution of the exchanged ions. Finally, the samples were heated at 673 K for 15 h.

A Perkin-Elmer DSC7 unit was used for the measurements.

A problem in measuring thermodesorption from zeolite by DSC is the choice of a suitable reference material [10]. Zeolite exhibits continuously changing heat capacities as a function of temperature, thus making the use of classical reference materials ambiguous [11]. Therefore, the solution is to perform the desorption run with Al metal as a reference and to maintain the sample at the end temperature until a stable signal is reached. The sample is cooled down without opening the cell and a 50 cm^3 min^{-1} NH_3–N_2 flow is applied for one hour. A nitrogen flow is re-applied and the sample is scanned at 10°C min^{-1} up to 600°C.

RESULTS AND DISCUSSION

Cationic large-port and small-port mordenites

Sodium large- and small-port mordenites show the same qualitative behaviour [12]. Three distinct desorption peaks were detected for both types. Although the amount desorbed above 350°C is nearly the same (Fig. 1), the energy required to desorb the last water molecule per unit cell from NaSPM is substantially larger. This can be explained by the prescence of pore-reducing entities; in small-port mordenite, these could prevent some Na ions from attaining the same degree of coordination to the structural oxygen atom as attained in large-port mordenite.

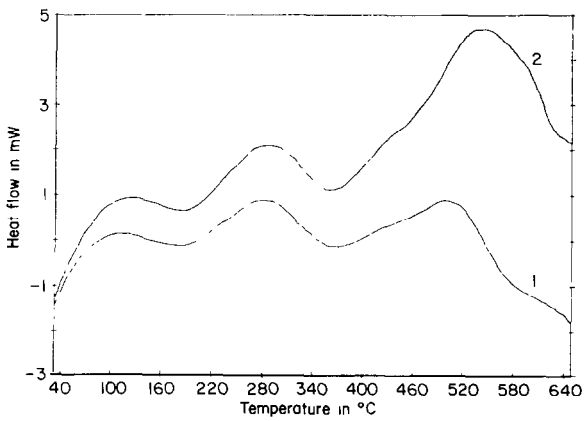

Fig. 1. DSC scans of (1) NaLPM and (2) NaSPM mordenites (2°C min^{-1}, N_2).

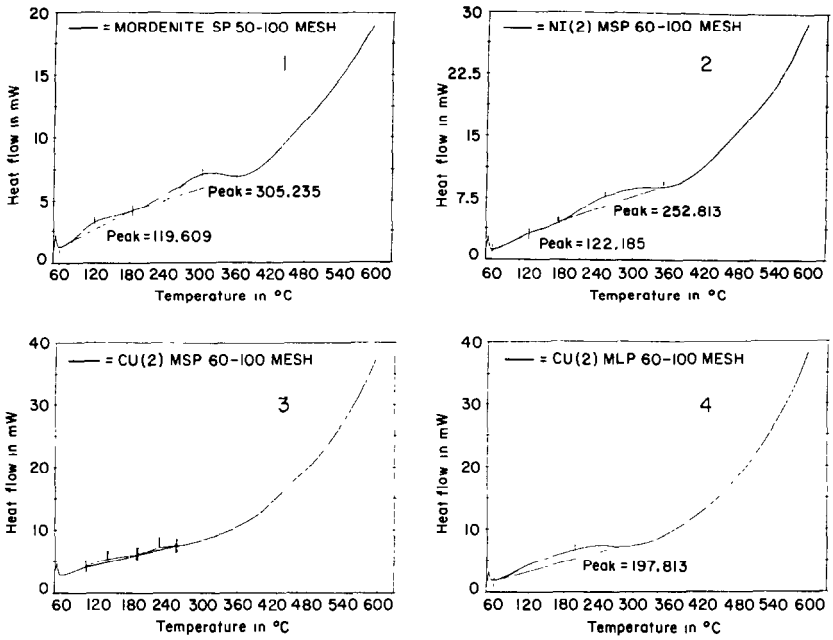

Fig. 2. DSC scans of ammonia desorption from: (1) NaSPM; (2) NiSPM; (3) CuSPM; (4) CuLPM.

DSC scans of ammonia desorption from NaSPM (Fig. 2) show two distinct endothermic peaks at 119 and 305°C. The first peak represents the physisorbed ammonia whereas the second peak represents the strong NH_3–Na^+ interaction of a Brønsted site, thus forming NH_4^+ Ions.

For both NiSPM and CuSPM (Fig. 2, (2) and (3)), the first peak in the DSC curve is similar in position to that found for NaSPM and can be ascribed to physisorbed ammonia. It is obvious that the amount of physisorbed ammonia is comparatively small compared with NaSPM. The presence of significant changes in ammonia physisorption confirms that major structural differences exist between the Na-mordenite form and the modified analogues.

The second peak of NH_3 chemisorption in the NiSPM and CuSPM samples, shows a maximum at 252°C for NiSPM and at 235°C for CuSPM. Thus, there is a shift to a lower temperature for the second endothermic peak for both the modified copper and nickel samples, compared with the parent NaSPM sample. This could be a consequence of the difference in the desorption energy of ammonia from cations located in the main channels and in the side pockets. The small amounts of ammonia desorbed at 235°C, in the case of CuSPM, may be due to the larger size of the Cu^{2+} ions and their lower solvation energies compared with Ni^{2+} ions. In addition, the high temperature peak at approx. 305°C for NaSPM, is assigned to an interaction between ammonia and sodium cations whereas the peak near

250°C reflects the coordination interaction between ammonia and framework aluminium. These results are in agreement with those of Topsoe et al. [13]. Furthermore, X-ray diffraction [14] results show that the sodium is evenly distributed over sites in large channels and side pockets. Therefore, we expect some of Na^+ ions to coordinate poorly with the structure upon desorption (first peak) and also to retain their strength at high temperatures to give the second peak.

The CuLPM sample shows one broad endothermic peak at 197°C compared with two peaks in the CuSPM sample.

Irrespective of whether one attributes the LP–SP difference to the presence of non-framework species or structural defects, the existence of pore-reducing entities within the large channel system must be acknowledged in order to explain the above behaviour. It is even conceivable that the entities, to a certain extent, have similar effects on the modifying agents as non-structural aluminimum, and shield the hydroxyls in the large channels, consequently slowing the cations and directing the reaction to the side pockets.

Accordingly, the catalysts under investigation can be arranged in order of decreasing acidity as NaSPM > NiSPM > CuSPM > CuLPM.

Y-zeolite

The DSC scans of NH_4 desorption from Cu–Y, Ni–Y and Co–Y are shown in Fig. 3. Two endothermic peaks are obtained for both Cu–Y and Ni–Y, whereas only one large endothermic peak, is observed for Co–Y.

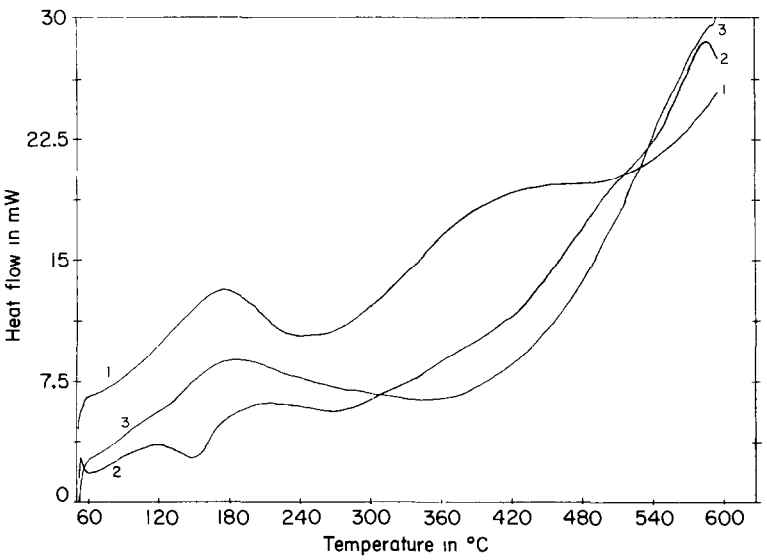

Fig. 3. DSC scans of ammonia desorption from : (1) CuY; (2) NiY; (3) CoY.

The representative DSC profiles of both Cu–Y and Ni–Y are quite different, reflecting the amount of ammonia desorption. Two endothermic peaks centred at 172 and 389°C are obtained for the Cu–Y sample whereas the Ni–Y sample shows peaks at 113 and 197°C. Such divergent behaviour indicates that copper cations which were originally located in the supercage can migrate to the small cages at elevated temperatures [15]. Moreover, copper ions are built into the small cage sites with greater ease than nickel ions [16], and the small cages sites are filled at 463 K for Cu^{2+} ions as opposed to 493 K for Ni^{2+} ions [15].

Furthermore, the increase in the electrostatic field associated with the copper ions, which results in a greater weakening of the O· · · H bond of the Brønsted acidity, can generate a strong acid function as a result of zeolite dehydration.

Therefore, we may assign the peak at 172°C, in case of Cu–Y, to the interaction of ammonia with extra-framework aluminium species, whereas the peak at 389°C is due to ammonia desorbed from Brønsted acid sites. In case of Ni–Y, the first peak at 113°C can be attributed to the physisorbed ammonia and to excess water, and the peak at 197°C can be assigned to coordinative interaction between ammonia and framework aluminium.

This difference in behaviour between Ni–Y and Cu–Y can also be attributed to the existence of specific extra-framework species for Ni^{2+}, which is doubtful for Y-zeolite [17]. Furthermore, Y-zeolites present a uniform distribution of strong acid sites, whereas this distribution is heterogeneous in mordenite zeolites. Therefore, the acidity strength of the second peak in Cu–Y is larger than that for CuSPM sample.

KINETICS INVOLVED DURING THERMODESORPTION OF AMMONIA FROM ZEOLITE SAMPLES

A desorption process from a surface material can be described by the Polanyi–Wigner equation [18]

$$\frac{d\theta}{dt} = k\theta^n \tag{1}$$

where θ is the degree of coverage, k is the rate constant and n is the reaction order. Read sorption can occur during the desorption process [19].

For an energetically homogeneous surface it is possible to combine eqn. (1) with the Arrhenius equation $k = A \exp(-E_a/RT)$ yielding

$$\frac{d\theta}{dt} = A \exp(-E_a/RT)\theta^n \tag{2}$$

In an isothermal, first-order desorption, this equation implies that plot of $\ln \theta$ versus time should yield a straight line with slope $-k$; from isothermal

TABLE 2

Parameters obtained for ammonia desorption from modified zeolites by DSC

	Mordenites						
	NaSPM	CuSPM	NiSPM	CuLPM	CuY	NiY	CoY
Peak range/°C (1st)	61.2–184.9	70–180	61.1–173	62–273	64.6–241.6	51.1–148	58–338
Peak range/°C (2nd)	184.9–365	180–270	172–349	–	265.6–496	148–266	–
Peak max./°C (1st)	119	129	122.1	197	172	113.5	176
Peak max./°C (2nd)	305	220	252.8	–	389.5	197	
ΔH/J g^{-1} (1st)	14.96	2.05	1.69	59.2	137.7	20	195
ΔH/J g^{-1} (2nd)	40.57	3.08	44.9	–	116.5	49.9	
E_a/kJ mol^{-1} (1st)	156.5	160.4	157.63	187.6	192.4	168.1	194.1
E_a/kJ mol^{-1} (2nd)	230.7	200.7	209.5	–	286.2	203.1	

runs at different temperatures, E_a and A can be evaluated using

$$\ln k = \ln A - E_a/RT \tag{3}$$

An alternative way to obtain desorption activation energies via temperature-programmed desorption was first proposed by Cvetanovic and Amenomiya [20]

$$2 \ln T_m - \ln B = E_a/RT + \ln(E_a/RA) \tag{4}$$

Equation (4) is derived from eqn. (2) by introduction of linear temperature programming, $T = T_0 + Bt$ where B is the heating rate, and T_m the desorption maximum, as a function of the heating rate.

This technique allows a rapid estimation of the average activation energy and A values and, in a number of cases, correlations have been found with structural changes [21].

Obtaining the activation energy from thermodesorption data is often arduous and can lead to ambiguous results. Therefore this type of analysis is limited to systems showing well-resolved peaks.

The activation energy values and the corresponding reaction heats, depicted as a function of ammonia desorption from different modified zeolite substrates, are shown in Table 2. It is obvious that the desorption activation energy values E_a, which are valuable quantitative data attributed to the relative proportions of different acid sites and their strength distributions, confirm the above explanation for the different behaviour of the zeolites, with the order of decreasing acidity obtained above: NaSPM > NiSPM > CuSPM and CuY ≫ NiY.

The difference in activation energies observed for both Cu–Y and Ni–Y reflects the difference in energy required to form a transition stage between the two lattice positions (sodalite and supercages) for the Cu–Y sample, while in the Ni–Y sample, it seems that such a transition is forbidden.

REFERENCES

1 K.M. Minachev, Y.I. Isakov and V.P. Kalinin, Proc. 5th Int. Zeolite Conf., Naples, Heyden, London, 1980, p. 866.
2 K. Mahos, R. Nakamura and H. Niijima, Proc. 7th Int. Zeolite Conf., Tokyo, Kodensha and Elsevier Publishers, Japan, 1986, p. 973.
3 P. Gallesot, Proc. 6th Int. Zeolite Conf., Reno, Butterworths, London, 1983, p. 352.
4 J.H. Lunsford, in J.R. Katzer (Ed.), Molecular Sieves-II. American Chemical Society, Washington, 1977, p. 473.
5 R.M. Barrer and L.V.C. Rees, Trans. Faraday Soc., 50 (1952) 852.
6 L.V.C. Rees and T. Berry, Molecular Sieves, Soc. Chem. Ind., London, 1986, p. 149.
7 Kh. Minachev and Ya I. Isakov, in J.A. Rabo (Ed.), Zeolites Chemistry and Catalysis, ACS Monograph 171; American Chemical Society, Washington, DC, 1976.
8 P. Chu and E.G. Deyer, ACS Symp. Ser., 59 (1983) 218.
9 D.P. Matthews and L.V.C. Rees, Chem. Age India, 37(5) (1985) 353.
10 J.J. Peter De Hulsters, Ph.D. Thesis, Univ. of Antwerp, 1990.

11 A.K. Aboul-Gheit, M.A. Al-Hajjaji and A.M. Summan, Thermochim. Acta, 19 (1987) 118.
12 A. Auroux, Y.S. Jin and J.C. Vedrine, Appl. Catal, 36 (1988) 323.
13 N.Y. Topsoe, K. Pedersen and E.G. Derouane, J. Catal., 70 (1981) 41.
14 J.L. Schlenker, J.J. Pluth and J.V. Smith, Mater. Res. Bull., 14 (1979) 751.
15 B. Goughlan and M.A. Keane, J. Chem. Soc. Faraday Trans., 86(6) (1990) 1007.
16 A. Barcicka and S. Pikus, Zeolites, 7 (1987) 35.
17 C.J.J. Den Ouden, R.A. Jackson, C.R.A. Catlow and M.F.M. Post, J. Phys. Chem., 94 (1990) 5286.
18 V. Dondur and D. Vucelic, Thermochim. Acta, 68 (1983) 91.
19 V. Dondur, D. Fidler and D. Vucelic, Proc. 7th Int. Conf. on Thermal Analysis: Vol II, Ontario, J. Wiley, New York, 1982, p. 1209.
20 R.J. Cvetanovic and Y. Amenomiya, Adv. Catal., 17 (1967) 103.
21 G.I. Kapustin, T.B. Brueva, A.L. Klyachko, S. Beran and B. Wichterlova, Appl. Catal., 42 (1988) 239.